Proceedings of ICRC 2001: 2403 © Copernicus Gesellschaft 2001

ICRC 2001

The size of the emission region of VHE gamma rays in the Crab Nebula

W. Hofmann and G. Pühlhofer, for the HEGRA collaboration

Max Planck Institut für Kernphysik, Postfach 103980, D-69029 Heidelberg, Germany

Abstract. The HEGRA system of imaging atmospheric Cherenkov telescopes provides for specially selected classes of events an angular resolution of better than 3'. By comparing the measured angular distribution of TeV gamma rays from the Crab Nebula with the distribution expected on the basis of Monte Carlo simulations, and with measurements of gamma rays from the point source Mrk 501, we conclude that the rms size of the VHE gamma-ray emission region in the Crab Nebula is less than 1.5'.

1 Introduction

The Crab Nebula is one of the best-studied objects in the sky, in all wavelength regimes. It has been established as a TeV gamma-ray source by the Whipple group, using the imaging atmospheric Cherenkov technique (Weekes et al. 1989, Vacanti et al. 1991), and has been studied with many other Cherenkov telescopes. The precise spectral shape of gamma-ray emission from the Crab Nebula has been the subject of a number of recent publications (Hillas et al. 1998, Tanimori et al. 1998, Aharonian et al. 2000a). The spectrum is consistent with a power-law extending from a few 100 GeV out to energies of 50 TeV and beyond. Contrary to observations in the X-ray and GeV gamma-ray regimes, the TeV gamma-ray emission does not show a pulsed component attributable to a direct contribution from the Crab Pulsar; pulsed emission is below 3% of the DC flux (Aharonian et al. 1999c, Burdett et al. 1999). The commonly accepted model for VHE gamma-ray production in the Crab Nebula assumes electron acceleration in the termination shock of thepulsar wind at a distance of about 0.1 pc (0.2') from the pulsar (see, e.g., Kennel & Coroniti (1984), De Jager & Harding (1992), Atoyan & Aharonian (1996), Aharonian & Atoyan (1998)). The electrons diffuse out into the Nebula and produce a characteristic two-component electromagnetic spectrum: synchrotron emission dominates at most energies up to about 0.1 GeV, whereas the inverse Compton process generates higher-energy gamma-rays with energies from the GeV range up to 100 TeV and beyond.

The Crab Nebula represents an extended source of electromagnetic radiation. Since the electrons loose energy as they expand out into the Nebula, primarily due to synchrotron losses, the effective source size is predicted to shrink with increasing energy of the radiation, with radio emission extending up to and beyond the filaments visible in the optical, whereas hard X-rays and multi-TeV gamma-rays should be produced primarily in the direct vicinity of the shock (see, e.g., Kennel & Coroniti (1984), De Jager & Harding (1992), Atoyan & Aharonian (1996), Amato et al. (1999)). At TeV energies, a second production mechanism for gamma-rays could be the hadronic production by protons accelerated in the shock (Atoyan & Aharonian 1996) or resulting from decays of secondary neutrons produced in the pulsar magnetosphere (Bednarek & Protheroe 1997); gamma rays are produced in interactions with the surrounding material, e.g. in the filaments (Atoyan & Aharonian 1996). Given that the size of the Crab Nebula – with its about 4' by 3' extension in the optical – is comparable to the angular resolution achieved for TeV gamma rays by the HEGRA system of imaging atmospheric Cherenkov telescopes (IACTs), a study of the size of the TeV emission region of the Crab Nebula is now possible with meaningful sensitivity. This paper reports such an analysis (see also Aharonian et al. (2000b)), based on data collected over the last years with the HEGRA IACT system.

The size of the Crab Nebula as a function of the energy of the radiation is summarized in Fig. 1, see Aharonian et al. (2000b) for details and references. A clear trend for decreasing source size with increasing energy is evident. Included as dashed line is the frequency dependence of the synchrotron emission region as sketched in Kennel & Coroniti (1984). The size of the emission region for inverse-Compton TeV gamma rays can be predicted using the average magnetic field to relate synchrotron photon energies to electron energies and to inverse-Compton gamma rays; from such ar-

Correspondence to: W. Hofmann
(Werner.Hofmann@mpi-hd.mpg.de)

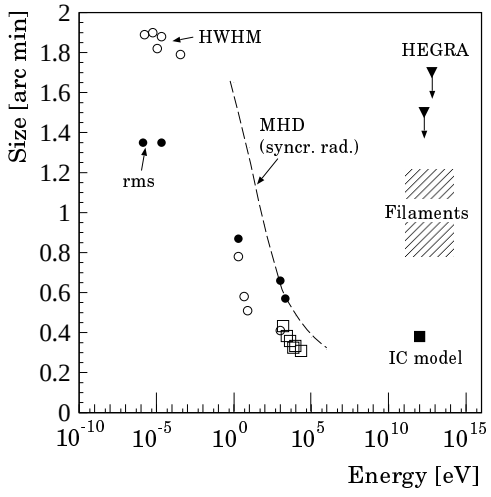

Fig. 1. Angular size of the Crab nebula at different frequencies. Full circles: rms size, averaged over directions. Open circles: half width at half maximum (HWHM, defined as FWHM/2), averaged over the long and short axis. Open squares: HWHM along the 300° direction. The dashed line indicates the frequency dependence of the size of the (synchrotron-radiation) emission region as given by Kennel & Coroniti (1984), and the full square shows the rms size predicted for inverse-Compton gamma-rays at TeV energy (Atoyan & Aharonian 1996). The dashed region indicates the rms size range of the filaments, the likely scale for hadronic production mechanisms. The triangles show the upper limits on the rms source size at TeV energies derived in this work.

guments, one concludes that the size for TeV gamma-rays should correspond to the X-ray size. The rms size predicted for the TeV gamma-ray emission region by the detailed calculations of Atoyan & Aharonian (1996) is included in Fig. 1. Basically, inverse-Compton TeV gamma-rays should emerge from the toroidal X-ray emission region clearly visible in the ROSAT data (Hester et al. 1995) and in the recent Chandra image (Weisskopf et al., 2000), as already speculated earlier by Aschenbach & Brinkmann (1975). The projected semi-major and semi-minor axes of the emission torus are 38" and 18", respectively. Due to the nonuniform strength of X-ray emission along the torus, the resulting emission profile is roughly elliptical, and its center is shifted relative to the pulsar location by about 0.3'. Hadronic production mechanisms are expected to generate larger source sizes, of the scale of the size of the nebula (shaded region in Fig. 1).

2 Observations of the Crab Nebula with the HEGRA CT system

The HEGRA system of imaging atmospheric Cherenkov telescopes is located on the Canary Island of La Palma, on the site of the Observatorio del Roque de los Muchachos. The telecope system consists of five telescopes, with a mirror area of 8.5 m^2 and a focal length of 5 m. Details about the HEGRA IACTs and their performance can be found in Daum et al. (1997), Aharonian et al. (1999b).

The Crab Nebula was observed in each season since the HEGRA IACT system commenced operation in late 1996, initially with three telescopes, later with four and since late 1998 with the complete set of five telescopes. Observations were carried out in the so-called wobble mode, with the source offset by 0.5° in declination relative to the telescope axes. The sign of the offset alternated every 20 min. A region offset by the same amount, but in the opposite direction, is used for background estimates, avoiding the need for special off-source observations.

The techniques for data analysis are similar to those documented, e.g., in Aharonian et al. (1999b,1999d). Direction and impact point of an air shower are reconstructed from the stereoscopic views of the shower. Based on the measured impact point and the known (Aharonian et al. 1999a) distribution of Cherenkov light as a function of the distance to the shower axis, an energy estimate is derived, with a typical resolution of 20%. Gamma-ray candidates are selected on the basis of image shapes.

In detail, the reconstruction of shower geometry differs somewhat from the techniques used so far. Whereas the normal reconstruction procedure combines images from all telescopes regardless of their quality, the new procedure assigns – on the basis of the Monte Carlo simulations of Konopelko et al. (1999) – errors to the relevant image parameters (the location of the image centroid and the orientation of the image axis). These errors depend on the intensity and the shape of the images and are propagated through the geometrical reconstruction, resulting in error estimates (or, to be precise, a covariance matrix) for the shower parameters. Details of the algorithm are given in Hofmann et al. (1999). Depending on the characteristics of an event, an angular resolution between 2' and more then 10' is predicted, with average value slightly below 6' [1]. The ability to select subsets of events with better-than-average resolution will be used extensively in the analysis of the size of the VHE emission region in the Crab Nebula.

3 Location of the VHE gamma-ray source

If indeed the VHE gamma ray emission correlates with X-ray emission, one would expect the center of gravity of the gamma-ray source to be shifted relative to the pulsar, as observed for X-rays. The expected shift is, however, comparable to the systematic pointing errors of the HEGRA telescopes, which are estimated to 25". The pointing of the telescopes is referenced to and corrected offline on the basis of star images (Pühlhofer et al. 1997), and the achievable pointing precision has been investigated in considerable detail (Pühlhofer et al. 2001). Fig. 2 shows the reconstructed source position superimposed to the Chandra image of the Crab Nebula (Weisskopf et al. 2000). The statistical errors

[1] Here and in the following, "angular resolution" is defined as the Gaussian width σ of the distribution of reconstructed shower directions, projected onto one axis of a local coordinate system.

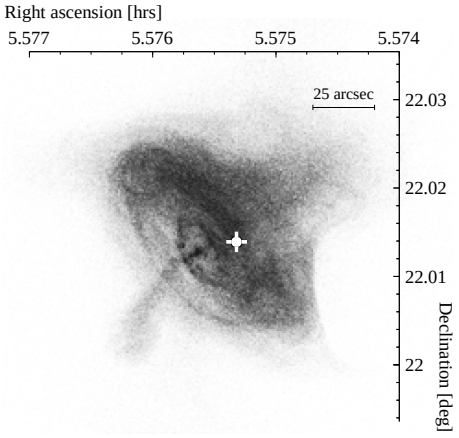

Fig. 2. Reconstructed location of the gamma-ray source in the Crab Nebula, superimposed to the Chandra X-ray image (courtesy of NASA/CXC/SAO). The error bars indicate statistical errors; the systematic error of 25" is also shown. The typical angular resolution for individual gamma rays (about 6') is larger than the shown coordinate system.

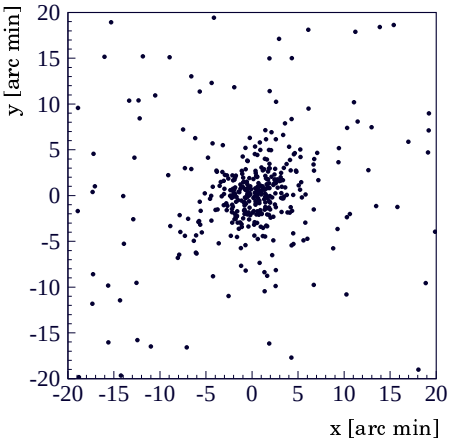

Fig. 3. Angular distribution of reconstructed showers in a local coordinate system centered on the Crab pulsar. Events were selected on the basis of the predicted angular error ($<$ 3' in both directions) and on the basis of image shapes (*mean scaled width* < 1.2).

on the source position are about 4". The gamma-ray source is indeed offset from the location of the pulsar; however, both a location of the source at the pulsar or near the torus are consistent with the data, given the systematic errors.

4 Limit on the size of the emission region

Even if the size at radio wavelengths – about 1.3' rms – is used as a most extreme possibility for the size at TeV energies, the source size σ_s is still smaller than the angular resolution σ_o for the best subsets - about 2' to 3'. Therefore, one cannot expect to generate a detailed map of the source. Instead, an extended emission region of (rms) size σ_s would primarily show up as a slight broadening of the angular distribution of gamma-rays, beyond the value determined by the experimental resolution. For an intrinsic resolution of 3' (in a projection) and a 1.5' rms source size, one would find a 3.4' wide angular distribution; for the 6' resolution, the resulting width is 6.2'. In order to positively detect a finite source size, or to derive stringent upper limits, one has (a) to measure the width of the angular distribution of gamma-rays with sufficient statistical precision, and (b) to quantitatively understand the response function of the instrument at the same level, and to control systematic effects which influence the resolution. If, e.g., the intrinsic resolution σ_0 of the instrument is known and reproducible to 10%, the minimum source size which can be reliably detected is $0.46\sigma_o$. To search for indications of an extended source, one will hence select the subset of events with best angular resolution, at some expense in event statistics. Among gamma-ray events, we find that about 1% of the events have a predicted resolution below 1.8' ($0.03°$), 6% below 2.4' ($0.04°$), 15% below 3' ($0.05°$), and 60% below 6' ($0.1°$), respectively. In particular the samples with resolutions better than 2.4' or 3' combine good angular resolution with acceptable statistics. Fig. 2 shows the angular distribution of events retained after a cut at 3' resolution in both projections, applying only very loose additional cuts on event shapes (a cut on the *mean scaled width* at 1.2, which retains over 80% of the gamma-ray events). The selection also biases the sample towards higher energies, since high-energy events produce more intense images, with smaller errors on the image parameters. In the overall data sample, the median energy of reconstructed events is 0.9 TeV; after a cut on the resolution at 3', this value rises to 2.0 TeV.

To evaluate the level at which the angular resolution is understood, we use the sample of gamma-rays from the AGN Mrk 501 as a reference set (see Aharonian et al. (1999b, 1999d) for details on this data set), assuming that Mrk 501 represents a point source. Table 1, columns 2,3 compare the measured angular distribution for different subsets of events with the Monte-Carlo predictions. 'Angular resolution' again refers to the Gaussian width of the projected angular distribution of events. Excellent agreement between data and Monte-Carlo is seen for all data sets. We note that the resolution estimates given by the reconstruction algorithm are low by 10% to 15%, for the samples selected for good resolution. The $\leq$ 2.4' sample, e.g., should show a 2.2' resolution, compared to the measured value of 2.46'. Given the relatively crude parametrization of image parameter errors used in the reconstruction (Hofmann et al., 1999), a deviation at this level is not unexpected, and in any case the effect is fully reproduced by the simulations.

After these preliminaries, we can now address the Crab data set. Table 1, cols. 4,5 list the widths of the distributions for the Crab gamma-rays, and the corresponding simulations. In general, we find, within the statistical errors, good agreement between the Crab and Mrk 501 data sets, and between

Table 1. Width of the angular distribution of events relative to the source, comparing the Mrk 501 and Crab data sets with Monte Carlo simulations using the measured gamma-ray energy spectrum as an input. Data sets are selected according to the estimate of the angular resolution, as provided by the shower reconstruction algorithm. The quoted width values are derived using a Gaussian fit to the projected angular distribution. For the last two rows of the table, only the central part of the distribution is fit; there are significant non-Gaussian tails (both in the Monte Carlo and in the data).

Selection on angular resolution [arc min]	Mrk 501 MC [arc min]	Mrk 501 data [arc min]	Crab MC [arc min]	Crab data [arc min]
≤ 2.4	2.43 ± 0.05	2.46 ± 0.06	2.41 ± 0.05	2.41 ± 0.14
≤ 3	2.81 ± 0.04	2.83 ± 0.05	2.81 ± 0.04	2.70 ± 0.10
≤ 6	3.58 ± 0.03	3.63 ± 0.04	3.64 ± 0.04	3.70 ± 0.09
all events	4.23 ± 0.04	4.26 ± 0.04	4.30 ± 0.04	4.37 ± 0.10

Crab data and Monte-Carlo.

Since the width of the angular distribution of gamma-rays from the Crab Nebula is consistent with the expected width, and with the width observed for Mrk 501, we can only give an upper limit on the source size. Taking into account the statistical errors on the Crab sample and on the reference samples, we find – following Caso et al. (1998) – 99% confidence level upper limits of 1.0' for the sample with a cut at 3' resolution, and 1.3' for the ≤ 2.4' sample. To be conservative, and since it was always planned to use the ≤ 2.4' sample as a safest compromise between statistical and systematic uncertainties, we adopt the 1.3' limit. Adding in additional systematic uncertainties due to pointing precision, we quote a final limit of 1.5' for the rms source size at a median energy of 2 TeV.Selecting events above 5 TeV, the limit is 1.7'. The limits obtained in this work are included in Fig. 1.

5 Concluding remarks

The size limits given in this work illustrate the precision which can nowadays be reached in TeV gamma-ray astrophysics; a number of potential galactic and extragalatic sources are predicted to be extended sources on this scale.

The limit on the size of the TeV emission region of the Crab Nebula is, by a factor around 4, larger than the size predicted by the standard inverse Compton models for gamma-ray production in the nebula. The limits, however, approach the sizes expected for hadronic production models, where high-energy gamma-rays are produced by nucleon interactions, more or less uniformly throughout the nebula.

Acknowledgements. We profited from discussions with O.C. De Jager both on the emission mechanism in the Crab Nebula, and on Crab data analysis. The support of the HEGRA experiment by the German Ministry for Research and Technology BMBF and by the Spanish Research Council CYCIT is acknowledged. We are grateful to the Instituto de Astrofisica de Canarias for the use of the site and for providing excellent working conditions. We gratefully acknowledge the technical support staff of Heidelberg, Kiel, Munich, and Yerevan.

References

Aharonian, F.A. & Atoyan, A.M., 1998, in 'Neutron Stars and Pulsars', S. Shibata & M. Sato, Eds., and astro-ph/9803091
Aharonian, F.A., Akhperjanian, A.G., Barrio, J.A., et al., 1999a, Astropart. Phys. 10, 21
Aharonian, F.A., Akhperjanian, A.G., Barrio, J.A., et al., 1999b, A&A 342, 69
Aharonian, F.A., Akhperjanian, A.G., Barrio, J.A., et al., 1999c, A&A 346, 913
Aharonian, F.A., Akhperjanian, A.G., Barrio, J.A., et al., 1999d, A&A 349, 11
Aharonian, F.A., Akhperjanian, A.G., Barrio, J.A., et al., 2000a, ApJ 539, 317
Aharonian, F.A., Akhperjanian, A.G., Barrio, J.A., et al., 2000b, A&A 361, 1073
Amato, E., Salvati, M., Bandiera, R., et al., 1999, submitted, and astro/ph-9911163
Aschenbach, B. & Brinkmann, W., 1975, A&A 41, 147
Atoyan, A.M. & Aharonian, F.A., 1996, Mon. Not. R. Astron. Soc. 278, 525
Bednarek, W. & Protheroe, R.J., 1997, Phys. Rev. Lett. 71, 2616
Burdett, A.M., Bond, I.H., Bolyle, P.J., et al., 1999, Proc. 26th ICRC, Salt Lake City, and astro-ph/9906318
Caso, C., Conforto, G., Gurtu, A., et al., 1998, Europ. Phys. J. C3, 1
Daum, A., Hermann, G., Heß, M., et al., 1997, Astropart. Phys. 8, 1
De Jager, O.C., & Harding, A.K., 1992, ApJ 396, 161
Hester,J.J., Scowen, P.A., Sankrit, R., et al., 1995, ApJ 448, 240
Hillas, A.M., 1985, Proc. 19th ICRC, La Jolla, Vol. 3, 445
Hillas, A.M., Akerlof, C.W., Biller, S.D., et al., 1998, ApJ 503, 744
Hofmann,W., Jung, I., Konopelko, A., et al., 1999, Astropart. Phys. 12, 135
Kennel, C.F. & Coroniti, F.V., 1984. ApJ 283, 710
Konopelko, A., Hemberger, M., Aharonian, A., et al., 1999, Astropart. Phys. 10, 275
Pühlhofer, G., Daum, A., Hermann, G., et al., 1997, Astropart. Phys. 8, 101
Pühlhofer, G., Kohnle, A., and Bolz, O., Technical performance of the HEGRA IACT system, these proceedings, 2001
Tanimori, T., Sakurazawa, K., Dazeley, S.A., et al., 1998, ApJ 492, L33
Vacanti, G., Cawley, M. F., Colombo, E., et al., 1991, ApJ 377, 467
Weekes, T.C., Cawley, M. F., Fegan, D. J., et al., 1989, Astrophys. J. 342, 379
Weisskopf, M.C., Hester, J.J., Tennant, A.F., et al., 2000, astro-ph/0003216